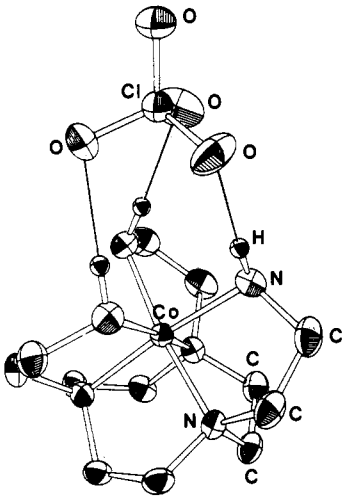

Figure 9. Structural view of $[Co(taetacn)](ClO_4)_3$ perpendicular to the C_3 axis, with capping perchlorate anion. Thermal ellipsoids enclose 50% probability. Data were obtained from ref 31b.

capped, then a structure not dissimilar to that of the cage complex $[Co(sep)]^{3+}$ is produced. The association between cation and anion bridges the three ligands and would serve to stabilize the complex, though to what degree is not known. If this stabilization is significant, then it is possible that the *lel*$_3$ and *lel*$_2$*ob* isomers are not subject to solvation or isomerization following reduction. Since the $[Co(pn)_3]^{3+}$ complexes in the *lel* configuration have the axially oriented N–H bonds, they are expected and found[32,33] to associate more strongly with tetrahedral anions than those adopting *ob* configurations. Consequently, the *ob*$_2$*lel* and *ob*$_3$ isomers will be less stabilized by association with perchlorate and therefore more subject to rearrangement or solvation, consistent with the apparently more complex reduction processes observed for these species. Finally, specific adsorption effects are indicated, which can affect the $E_{1/2}$ values. Adsorption effects can be strongly influenced by the configuration. The importance of the concepts described in this paper is also very relevant to enantiomer differentiation effects on the reduction of racemic tris(acetylacetonato)cobalt(III) complexes and related species in the presence of optically active electrolytes.[37]

Conclusions

The electrochemical reduction of complexes containing configurational isomers cannot be treated as a single electrode process of the kind

$$Co(III) + e^- \overset{E^\circ,\, k_s,\, \alpha}{\rightleftharpoons} Co(II)$$

Unfortunately, a realistic kinetic treatment of a system containing a wide range of configurations cannot be undertaken without a knowledge of numerous variables in both oxidation states, which must be obtained by independent measurements. In the case of $[Co\{(\pm)\text{-}pn\}_3]^{2+}$, no data are available on the distribution of the configurations except for theoretical information from molecular mechanics, which does not allow for ion pairing and related terms. Even if this information were available, numerous unknown E° values, k_s values, and α values need to be coupled with all the equilibrium constants to provide an essentially intractable problem. The theoretical calculations predict that a range of E° values spanning an approximately 20 mV potential range will be observed for the $[Co\{(\pm)\text{-}pn\}_3]^{3+/2+}$ system. Experimental data are consistent with this prediction. In other systems, crystallographic data are available which confirm that configurational changes accompany electron transfer,[38,39] although the influence of this phenomenon still has been treated by the simple models depicted by eq 1 and 2. The present work confirms that a complete understanding of electron transfer and structural changes accompanying electron transfer is still not available[5,40] and that further theoretical studies on conformational[41] (configurational) aspects of redox reactions are still required.

Registry No. *fac*-$[Co\{(\pm)\text{-}pn\}_3]^{3+}$, 46469-36-7; *mer*-$[Co\{(\pm)\text{-}pn\}_3]^{3+}$, 46469-26-5; *fac*-$[Co\{(\pm)\text{-}pn\}_3]^{2+}$, 108509-36-0; *mer*-$[Co\{(\pm)\text{-}pn\}_3]^{2+}$, 108509-37-1; Bu_4NClO_4, 1923-70-2; Bu_4NPF_6, 3109-63-5; Hg, 7439-97-6.

(37) Yoshinaga, K.; Kito, T.; Okhubo, K. *Nippon Kagaku Kaishi* **1986**, 165 and references cited therein.
(38) Küppers, H.-J.; Neves, A.; Pomp, C.; Ventur, D.; Weighardt, K.; Nuber, B.; Weiss, J. *Inorg. Chem.* **1986**, *25*, 2400.
(39) Connor, K. A.; Gennett, T.; Weaver, M. J.; Walton, R. A. *J. Electroanal. Chem. Interfacial Electrochem.* **1985**, *196*, 69.
(40) Geiger, W. E. *Prog. Inorg. Chem.* **1985**, *33*, 275.
(41) Tosi, C.; Fusco, R.; Ranghino, G.; Malatesta, V. *J. Mol. Struct.* **1986**, *134*, 341.

Contribution from the Department of Chemistry, The University of Calgary, Calgary, Alberta, Canada T2N 1N4

Alkali Metal Ion, Temperature, and Pressure Effects on the Rate of Electron Transfer between Manganate(VI) and Permanganate(VII) Ions in Alkaline Aqueous Solution

Leone Spiccia and Thomas W. Swaddle*

Received January 23, 1987

The rate of outer-sphere electron transfer between MnO_4^- and MnO_4^{2-} in aqueous MOH at constant ionic strength (1.1 mol L^{-1}) is given by $(k_0 + k_M[M^+])[MnO_4^-][MnO_4^{2-}]$, where k_0 is defined by the activation parameters $\Delta H_0^* = 46$ kJ mol^{-1}, $\Delta S_0^* = -35$ J K^{-1} mol^{-1}, $\Delta V_0^{\circ *}$(0.1 MPa, 318 K) = −23 cm^3 mol^{-1}, and $\Delta\beta_0^* \simeq -0.06$ cm^3 mol^{-1} MPa^{-1}. For M = Li, Na, K, and Rb, respectively, k_M is given by $\Delta H_M^* = 33.1$, 32.2, 32.9, and 32.9 kJ mol^{-1} and $\Delta S_M^* = -67.8$, −68.4, −62.9, and −59.0 J K^{-1} mol^{-1}, while, for M = Na and K, $\Delta V_M^* = +3$ and −1 cm^3 mol^{-1}. The activation parameters for the cation-independent reaction pathway can be accounted for by a modified semiclassical Marcus–Hush theory if, in the transition state for adiabatic or nearly adiabatic electron transfer, the reacting ions are taken to be enclosed within a common cavity in the solvent and the Mn–Mn distance compresses as does the cavity, which is assumed to have the same compressibility as the solvent itself. The lower enthalpies, and markedly more positive volumes, of activation for the M^+-catalyzed pathway appear to arise at least in part from an easing of these solvational constraints.

Introduction

Wherland[1] has pointed out that the apparent success of Stranks' adaptation[2] of the classical Hush–Marcus theory[3–6] of outer-sphere electron-transfer (OSET) reaction rates to cover pressure effects was fortuitous; there was an error in the sign of the term representing the contribution of ionic medium (Debye–Hückel) effects.

(1) Wherland, S. *Inorg. Chem.* **1983**, *22*, 2349.
(2) Stranks, D. R. *Pure Appl. Chem.* **1974**, *38*, 303.
(3) Marcus, R. A. *J. Chem. Phys.* **1956**, *24*, 966, 979.
(4) Marcus, R. A. *J. Chem. Phys.* **1957**, *26*, 867.
(5) Marcus, R. A. *Discuss. Faraday Soc.* **1960**, *29*, 21.
(6) Hush, N. S. *Trans. Faraday Soc.* **1961**, *57*, 557.

0020-1669/87/1326-2265$01.50/0 © 1987 American Chemical Society

In reality, the few experimental volumes of activation ΔV^* currently available for symmetrical electron-transfer (self-exchange) reactions of established outer-sphere mechanism are all more negative than the corrected Stranks theory would predict.[1,7] It is therefore appropriate not only to reexamine the theory of pressure effects on OSET rates[7-9] but to seek ΔV^* data for further self-exchange reactions to test it.

The manganate–permanganate exchange reaction in aqueous alkali[9-14] is attractive in the following respects: it differs in charge type from the cation–cation self-exchange reactions studied under pressure to data,[7] it has already been mapped out at ambient pressure and shown to proceed by an outer-sphere mechanism,[10-14] it is amenable to study at high pressures by ^{55}Mn NMR techniques,[9,13,14] and the Mn–O bond distances for MnO_4^- and MnO_4^{2-} *in solution* are accurately known.[15] Furthermore, both adiabatic[4] and nonadiabatic[16] theoretical treatments of this reaction have been published. On the other hand, although it is evident[9-14] that the reaction rate is sensitive to the nature of the counterion that is present, as is typical of OSET reactions between ions of like sign,[17,18] the effects of cations on the rate of the manganate–permanganate exchange have not heretofore been characterized quantitatively except for the case of cesium ion, which causes a spectacular acceleration.[11] We have therefore examined the effects of metal ions $M^+ = Li^+$, Na^+, K^+, and Rb^+ at various temperatures and of hydrostatic pressures up to 180 MPa (for $M^+ = Na^+$ and K^+) on the manganate–permanganate self-exchange rate in aqueous alkaline media of constant ionic strength.

Experimental Section

Reagents. All manganate and permanganate salts were analyzed by titration with sodium oxalate. Potassium permanganate (99.8%) was obtained by recrystallization of the Fisher ACS Certified reagent from water, and potassium manganate (99.2%) was made by the method of Scholder and Waterstradt.[19] Sodium permanganate trihydrate (Aldrich) was purified (99.1%) by recrystallization twice from water. Sodium manganate decahydrate (97.5%) was made by heating 40 g of $NaMnO_4 \cdot 3H_2O$ and 50 g of NaOH in 100 mL water with stirring and filtering the hot solution into a plastic vessel; the green crystals that separated on cooling were washed with 0.5% aqueous NaOH. Lithium permanganate trihydrate (99.3%) was made by mixing equal volumes of saturated $NaMnO_4$ and 12 mol L^{-1} LiCl solutions. Rubidium permanganate was prepared by mixing filtered solutions of sodium permanganate trihydrate (10 g in 20 mL of water) and RbCl (K&K, 6.2 g in 10 mL of water) and recrystallizing the precipitate twice from water. Lithium hydroxide (98.5%) was obtained by mixing solutions of NaOH (42 g in 100 mL of water) and lithium acetate dihydrate (150 g in 50 mL of water) and recrystallizing the solid product twice from water.

Other reagents were obtained commercially and recrystallized from water where possible; otherwise, they were used as received. Distilled water was redistilled from alkaline $KMnO_4$ and again from potassium dichromate, but D_2O (Bio-Rad, 99.75% isotopic purity) was used without further treatment.

Preparation of Solutions. Solutions of appropriate weights of the requisite permanganate salt in 50% (by volume) H_2O/D_2O were filtered through a sintered-glass funnel of 4-μm porosity to remove any MnO_2 (this was essential to ensure the reproducibility of the NMR results) and then standardized with sodium oxalate prior to prompt use in making up solutions for the NMR experiments. The manganate solutions were prepared by dissolving the solid potassium manganate or sodium manganate in the appropriate standardized aqueous alkali containing any desired supporting electrolytes, and as with the permanganates, the solutions were filtered prior to standardization with sodium oxalate and prompt use in NMR line width measurements.

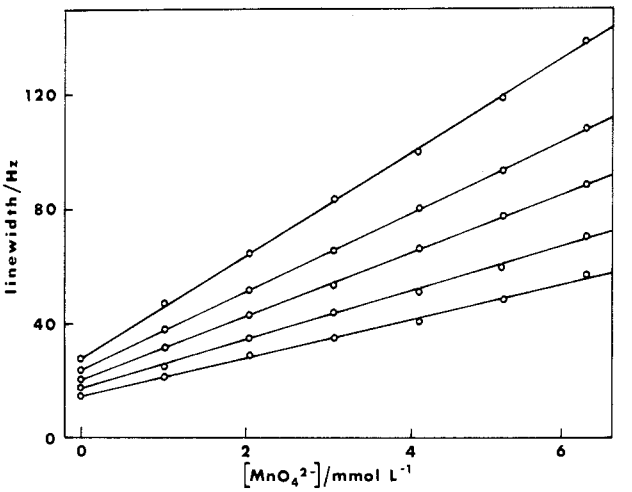

Figure 1. Dependence of $^{55}MnO_4^-$ line width $\Delta\nu_{1/2}$ on the K_2MnO_4 concentration at temperatures (from top line downwards) 62.0, 55.6, 50.8, 44.7, and 39.0 °C; $[Rb^+]$ = 1.107 mol L^{-1}; $[OH^-]$ = 0.2 mol L^{-1}; $[Cl^-]$ = 0.886 mol L^{-1}.

Solutions for NMR line width determinations were made by thoroughly mixing equal volumes of the appropriate manganate and permanganate solutions and, so, contained 25% D_2O as the signal locking material; it was established, through use of a solution in 100% H_2O with a D_2O insert, that the presence of 25% D_2O had not measurable effect on the line widths. For studies in which the manganate ion concentration was varied, sodium sulfate or potassium sulfate (as appropriate) was added to the manganate solution such that the total of manganate and sulfate concentrations was constant. For studies of the effect of varying the concentration of the cation M^+, various concentrations of MCl, MCl + M_2SO_4, M_2SO_4, or M_3PO_4 were employed so as to maintain the stoichiometric ionic strength at 1.1 mol L^{-1} (volume concentrations cited are as at ambient temperature and pressure, 294 K and 0.1 MPa). Phosphate was not used with M = Li or Rb. These studies could not be extended to include M = Cs because of the low solubility of some of the required cesium salts.

NMR Measurements. All measurements were made on a Bruker Model WH-90 (2.114 T, 22.285 MHz, ^{55}Mn) spectrometer with quadrature detection, in the deuterium locking mode. For studies at atmospheric pressure, the solutions were contained in spinning 10-mm NMR tubes, thermostated with flowing nitrogen, and the sample temperature was measured with a copper–constantan thermocouple that was calibrated against a standardized quartz thermometer. Temperatures were constant and reproducible to ±0.2 K. Spectra were collected with 400–5000 pulses of length 10 μs, delay time 200 μs, and sweep width 2.5–50 kHz, over 1024 data points. Line widths $\Delta\nu_{1/2}$ at peak half-height were calculated with the NCTFT program of the spectrometer's Nicolet 294 data-processing system.

NMR spectra at elevated pressures were obtained with a static probe generally similar to those described elsewhere,[20,21] but in which the pressure vessel was made of berylco-25 alloy, temperature measurement was made with a built-in calibrated platinum resistance thermometer, and the coil and matching circuits were designed for operation at 22 MHz. The sample was contained in a Teflon sample tube with a free piston of the same material. The temperature was controlled to within ±0.1 K with methanol from an external circulating thermostat. The shim settings were obtained by tuning on the sample's internal D_2O while locking on the probehead's external D_2O lock system; line widths for MnO_4^- alone were typically 20–25 Hz at room temperature and pressure with this procedure. Optimum spectrometer parameters were as follows: pulse width, 20–25 μs; number of scans, 2500; sweep width, 5 kHz; delay time, 750–850 μs.

Results

Variable-Temperature Studies. In accordance with previous studies,[13,14,22,23] it was confirmed (e.g., Figure 1) that the line width

(7) Swaddle, T. W. In *Inorganic High Pressure Chemistry: Kinetics and Mechanisms*; van Eldik, R., Ed.; Elsevier: Amsterdam, 1986; Chapter 5.
(8) Swaddle, T. W.; Spiccia, L. *Physica B+C (Amsterdam)* **1986**, *139/140B+C*, 684.
(9) Spiccia, L.; Swaddle, T. W. *J. Chem. Soc., Chem. Commun.* **1985**, 67.
(10) Sheppard, J. C.; Wahl, A. C. *J. Am. Chem. Soc.* **1957**, *79*, 1020.
(11) Gjertsen, L.; Wahl, A. C. *J. Am. Chem. Soc.* **1959**, *81*, 1572.
(12) Wahl, A. C. *Z. Elektrochem.* **1960**, *64*, 90.
(13) Myers, O. E.; Sheppard, J. C. *J. Am. Chem. Soc.* **1961**, *83*, 4739.
(14) Britt, A. D.; Yen, W. M. *J. Am. Chem. Soc.* **1961**, *83*, 4516.
(15) Sham, T. K.; Brunschwig, B. S. *J. Am. Chem. Soc.* **1981**, *103*, 1590.
(16) Dolin, S. P.; Dogonadze, R. R.; German, E. D. *J. Chem. Soc., Faraday Trans. 1* **1977**, *73*, 648. German, E. D., personal communiction.
(17) Rampi Scandola, A.; Scandola, F.; Indelli, A. *J. Chem. Soc., Faraday Trans. 1* **1985**, *81*, 2967.
(18) Bruhn, H.; Nigam, S.; Holzwarth, J. F. *Faraday Discuss. Chem. Soc.* **1982**, *74*, 129.
(19) Scholder, V. R.; Waterstradt, H. *Z. Anorg. Allg. Chem.* **1954**, *277*, 172.
(20) Ducommun, Y.; Newman, K. E.; Merbach, A. *Inorg. Chem.* **1980**, *19*, 3696.
(21) Sisley, M. J.; Yano, Y.; Swaddle, T. W. *Inorg. Chem.* **1982**, *21*, 1141.

Table I. Rate Constants and Thermal Activation Parameters for Electron Transfer between MnO_4^- and MnO_4^{2-} by Pathways Involving the Counterions M^+[a]

	M^+				
	Li^+	Na^+	K^+	Rb^+	Cs^+
ΔH_M^*/kJ mol^{-1}	33.1 ± 0.6	32.2 ± 0.7	32.9 ± 0.7	32.9 ± 0.3	
ΔS_M^*/J K^{-1} mol^{-1}	−67.8 ± 1.9	−68.4 ± 2.3	−62.9 ± 2.2	−59.0 ± 0.9	
$k_M/10^3$ L^2 mol^{-2} s^{-1} (0 °C)	0.77 ± 0.20	1.06 ± 0.32	1.51 ± 0.46	2.41 ± 0.29	12.0 ± 3.0[b]
$k_M/10^3$ L^2 mol^{-2} s^{-1} (25 °C)	2.84 ± 0.72	3.8 ± 1.1	5.6 ± 1.7	8.9 ± 1.1	
$k_M/10^3$ L^2 mol^{-2} s^{-1} (45 °C)	7.0 ± 1.8	9.2 ± 2.8	13.6 ± 4.1	21.8 ± 2.6	

[a] Ionic strength 1.1 mol L^{-1}; [OH^-] = 0.20 mol L^{-1}; concentration standard 1 mol L^{-1} at 294 K and 0.1 MPa. Values of, and uncertainties in, k_M are calculated from ΔH_M^* and ΔS_M^* except for M = Cs. [b] Reference 11.

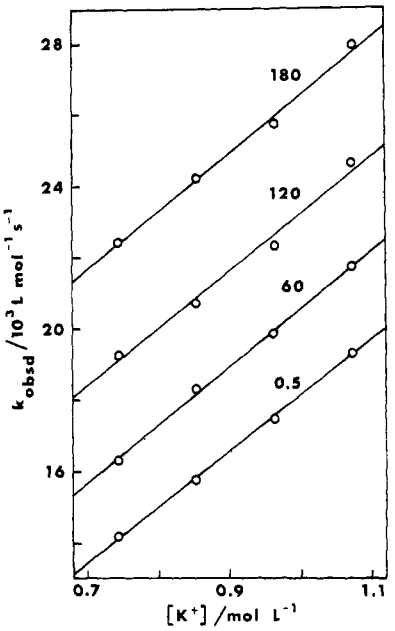

Figure 2. Dependence of k_{obsd} on potassium ion concentration at ionic strength 1.105 mol L^{-1}, 45.0 °C, and 60-MPa pressure intervals from 0.5 to 180 MPa.

of the $^{55}MnO_4^-$ resonance was a linear function of the relatively small concentration of the paramagnetic manganate ion present (for a fixed concentration of the counterion):

$$(\pi\Delta\nu_{1/2})_{P+D} = (\pi\Delta\nu_{1/2})_D + k_{obsd}[MnO_4^{2-}] \quad (1)$$

where subscripts P and D refer to the paramagnetic and diamagnetic manganese anions and k_{obsd} is the second-order rate coefficient for electron transfer under the particular reaction conditions.

$$-d[MnO_4^-]/dt = k_{obsd}[MnO_4^-][MnO_4^{2-}] \quad (2)$$

When the M^+ (M = Na or K) concentration was varied at constant ionic strength, k_{obsd} was found to be a linear function of the stoichiometric [M^+], within the experimental uncertainty (cf. Figure 2); thus, we have

$$k_{obsd} = k_0 + k_M[M^+] \quad (3)$$

The same relationship held for M = Li and Rb, but in those cases a small correction for the contribution of (respectively) the Na^+ and K^+, introduced with the MnO_4^{2-}/SO_4^{2-}, had to be applied. Unfortunately, the restriction of maintenance of constant ionic strength limited the range of [M^+] to about 0.7–1.1 mol L^{-1}, and furthermore the k_M term was predominant in all cases at ambient pressure (especially for M = Rb), so that typical standard deviations in the k_0 values ranged from 15% for M = Li to 37% for M = Rb, and accordingly the uncertainties in the enthalpies of activation ΔH_0^* were 3–4 kJ mol^{-1}. Full details of the measurements are collected in the supplementary tables; it suffices to note here that interpolated k_0 values at a chosen temperature were effectively the same for M = Li, Na, K, and Rb (e.g., at 298.2 K, $k_0/10^2$ L mol^{-1} s^{-1} = 6.7, 8.2, 6.9, and 7.8 respectively; mean 7.4 ± 0.7)—as, indeed, is expected if k_0 is a true rate constant reflecting the existence of an OSET pathway that is independent of M^+. Accordingly, all the k_0 data for M = Li, Na, and K (except for the K data points at 316.3 and 328.2 K, which lay slightly outside the 95% confidence limits of the consolidated fit) were combined to derive the corresponding enthalpy of activation ΔH_0^* = 46.3 ± 2.2 kJ mol^{-1} and entropy of activation ΔS_0^* = −34.6 ± 6.9 J K mol^{-1} for the M^+-independent OSET pathway, which give k_0 = 124, 749, and 2.59 × 10^3 L mol^{-1} s^{-1} at 0, 25.0, and 45.0 °C, respectively. These activation parameters in turn were used to calculate improved values of k_M from k_{obsd} (eq 3), and thence the ΔH_M^* and ΔS_M^* data given in Table I.

Table II. Pressure Dependence of the Cation-Dependent (k_M) and -Independent (k_0) Pathways for the Manganate–Permanganate Electron-Transfer Reaction[a]

	sodium		potassium	
press./MPa	$k_0/10^3$ L mol^{-1} s^{-1}	$k_{Na}/10^3$ L^2 mol^{-2} s^{-1}	$k_0/10^3$ L mol^{-1} s^{-1}	$k_K/10^3$ L^2 mol^{-2} s^{-1}
0	(3.0 ± 2.2)	10.1 ± 2.5	2.6 ± 0.4	15.5 ± 0.4
20	4.2 ± 1.0	9.3 ± 1.0	3.3 ± 0.5	16.1 ± 0.5
40	4.1 ± 1.2	10.1 ± 1.3	3.9 ± 0.1	15.8 ± 0.1
60	5.4 ± 0.6	9.9 ± 0.7	4.2 ± 0.6	16.3 ± 0.6
80	6.0 ± 1.0	9.4 ± 1.1	4.8 ± 0.4	16.7 ± 0.4
100	7.1 ± 1.1	9.1 ± 1.2	5.6 ± 1.0	16.9 ± 1.1
120	7.7 ± 0.7	9.4 ± 0.8	6.7 ± 1.8	16.6 ± 1.4
140	8.2 ± 1.1	9.4 ± 1.1	8.3 ± 0.3	16.2 ± 0.3
160	11.3 ± 0.7	7.2 ± 0.8	8.3 ± 0.6	17.1 ± 0.6
180	11.8 ± 0.7	7.3 ± 0.8	10.1 ± 0.8	16.5 ± 0.8

[a] 45.0 °C; ionic strength 1.11 mol L^{-1}; [OH^-] = 0.20 mol L^{-1}; concentration standard 1 mol L^{-1} at 294 K and 0.1 MPa.

Direct comparison of the present results with most of those obtained by Wahl, Sheppard, and co-workers[10-13] by both NMR and radiochemical methods is complicated by differences in conditions, notably ionic strength, and the need for a long extrapolation in temperature. The data of Table I predict k_{obsd} = 1.18 × 10^3 L mol^{-1} s^{-1} for [Na^+] = 1.00 mol L^{-1} at 0 °C, which is in excellent agreement with Britt and Yen's[14] pulsed-NMR value of (1.23 ± 0.25) × 10^3 and acceptably close to the 1.70 × 10^3 reported by Sheppard and Wahl[10] for these conditions. It is now evident, however, that it is incorrect to identify the value of k_{obsd} = 710 L mol^{-1} s^{-1}, measured in 0.16 mol L^{-1} NaOH,[10] with the cation-independent OSET rate coefficient k_0 at 0 °C; the similarity of k_{obsd} for the cases where M is Li and Na is due, not to k_M being negligible, but to the closeness of the values of k_{Li} and k_{Na}.

High-Pressure Studies. Line-broadening studies at pressures ranging from 0 to 180 MPa in 20-MPa intervals were carried out for M = Na and K at four different concentrations, first with increasing and then with decreasing pressure to obviate any hysteresis. The resulting k_{obsd} data (40 data points for each M) are collected in the supplementary tables.

Two methods of analysis of these data were used, giving results that were mutually consistent and rate constants for atmospheric pressure that were in satisfactory agreement with those for the variable-temperature study. The first procedure used the fact that k_{obsd} was again a linear function of [M^+] at any given pressure,

(22) McConnell, H. M.; Weaver, H. E., Jr. *J. Chem. Phys.* **1956**, *25*, 307.
(23) McConnell, H. M.; Berger, S. B. *J. Chem. Phys.* **1957**, *27*, 230.

Table III. Volumes of Activation and Zero-Pressure Rate Constants[a]

	M = Na	M = K
Pressurewise Analysis (Eq 4a,b)		
ΔV_o^*/cm^3 mol^{-1} [b]	−19.2 ± 1.1	−19.3 ± 0.8
ΔV_M^*/cm^3 mol^{-1} [b]	+4.2 ± 1.2	−0.9 ± 0.3
$k_o^0/10^3$ L mol^{-1} s^{-1}	3.3 ± 0.2	2.8 ± 0.1
$k_M^0/10^3$ L^2 mol^{-2} s^{-1}	10.4 ± 0.5	15.9 ± 0.2
All Data Taken Together (Eq 6)		
ΔV_o^{0*}/cm^3 mol^{-1}	−23.9 ± 5.3	−22.8 ± 4.9
ΔV_o^*/cm^3 mol^{-1} [b]	−20.5 ± 5.3	−20.4 ± 4.9
$\Delta\beta_o^*/10^2$ cm^3 mol^{-1} MPa^{-1}	−7.8 ± 3.2	−5.5 ± 2.9
ΔV_o^*/cm^3 mol^{-1} [b]	+2.3 ± 1.6	−1.4 ± 0.8
$k_o^0/10^3$ L mol^{-1} s^{-1}	3.4 ± 0.5	2.8 ± 0.4
$k_M^0/10^3$ L^2 mol^{-2} s^{-1}	9.7 ± 0.6	15.5 ± 0.5
"Best" Values		
ΔV_o^{0*}/cm^3 mol^{-1}	−22.8 ± 1.2	
ΔV_o^*/cm^3 mol^{-1} [b]	−20.0 ± 0.7	
$\Delta\beta_o^*$/cm^3 mol^{-1} MPa^{-1}	−0.06 ± 0.03	
$k_o^0/10^3$ L mol^{-1} s^{-1}	2.9 ± 0.4	
ΔV_M^*/cm^3 mol^{-1} [b]	+3.3 ± 1.0	−1.1 ± 0.3
$k_M^0/10^3$ L^2 mol^{-2} s^{-1}	10.1 ± 0.6	15.6 ± 0.5

[a] 45.0 °C; ionic strength 1.1 mol L^{-1}. [b] Average value over the range 0–180 MPa; all other data refer to 0.1 MPa.

as exemplified by Figure 2, which also shows clearly that, as the pressure was increased, the k_0 component (i.e., the intercept) was strongly accelerated while k_M (the slope) was only slightly affected. Thus, the fraction of k_{obsd} due to k_0 was larger and the derived k_0 values were somewhat more reliable in the high-pressure studies than in the variable-temperature work, especially for M = K (Table II; the k_0 values for M = Na are generally slightly larger than for the corresponding cases with M = K, but they agree within the error limits, and a systematic error in k_0 will not affect ΔV_0^*). The experimental uncertainty in k_0 is nevertheless still fairly large, so that simple linear relationships between ln k_0 or ln k_M and the pressure P

$$\ln k_0 = \ln k_0^\circ - P\Delta V_0^*/RT \quad (4a)$$

$$\ln k_M = \ln k_M^\circ - P\Delta V_M^*/RT \quad (4b)$$

seem adequate, but data scatter probably conceals the significant pressure dependence of ΔV_0^* predicted by theory (see Discusion). The volumes of activation ΔV_0^* and ΔV_M^* obtained by this pressurewise analysis and given in Table III should therefore be regarded as mean values for the pressure range 0–180 MPa. If, however, we introduce a nonzero but constant compressibility coefficient of activation $\Delta\beta_0^* = -(\partial\Delta V_0^*/\partial P)_T$ for the cation-independent pathway in analysis of either the Na or the K data set

$$\ln k_0 = \ln k_0^\circ - P\Delta V_0^{\circ *}/RT + P^2\Delta\beta_0^*/2RT \quad (5)$$

a zero-pressure volume of activation $\Delta V_0^{\circ *}$ of −22 ± 4 cm^3 mol^{-1} is obtained from eq 5, with $\Delta\beta_0^* = -0.03 \pm 0.03$ cm^3 mol^{-1} MPa^{-1}, which is statistically ill-defined but not negligible. The volumes of activation for the cation-dependent pathways are relatively small, and any pressure dependence they may have should be negligible. The values of k_0° and k_M° agree satisfactorily with those interpolated from the variable-temperature experiments (Table I), within the stated error limits.

The second statistical procedure involved taking all the data together for either M = Na or K and fitting them by a nonlinear least-squares method to

$$k_0 = k_0^\circ \exp[(-P\Delta V_0^{\circ *} + P^2\Delta\beta_0^*/2)/RT] + k_M^\circ \exp[-P\Delta V_M^*/RT] \quad (6)$$

In this case, the pressure dependence of ΔV_0^* cannot be ignored; otherwise, inconsistent kinetic parameters and a nonrandom distribution of residuals result. The results of this computation are also given in Table III. The close agreement between the ΔV_0^* or $\Delta V_0^{\circ *}$ values for M = Na and M = K, regardless of the mode of computation, and also the satisfactory agreement of the k_0° and k_M° values with corresponding data obtained in the variable-temperature experiments, give us confidence in the "best values" for the pressure activation parameters given at the bottom of Table III. (Our preliminary report[9] of $\Delta V_0^* = -21$ cm^3 mol^{-1} reflected a minor systematic error, now eliminated.)

Possible Effect of Ion Pairing. An obvious defect of the procedure of using variable amounts of anions of different charges to allow [M$^+$] to be adjusted while constant ionic strength is ostensibly maintained is that ion pairing by anions other than the reactants may reduce both the effective concentration of the free cation M$^+$ and, less significantly, the ionic strength itself. In order to gauge the possible importance of this effect, an attempt to adjust [M$^+$] for ion pairing was made on the basis of Fuoss' equation (1958 version, adapted for ionic strength 1.1 mol L^{-1} by incorporating the extended Debye–Hückel equation)[24] with allowance for the pressure and temperature dependences of the relative permittivity of water[25] and with ionic contact distances taken or estimated from those of Sørensen et al.[26]

The most significant effects of this adjustment were to reduce k_0 to some 50–60% of the value obtained by neglecting ion pairing and to make ΔV_0^* 6 cm^3 mol^{-1} more negative; k_{Na} and k_K became slightly (ca. 15%) larger, but ΔV_M^* was not materially changed, and in no case was the change in ΔH^* or ΔS^* greater than the experimental uncertainty in those quantities. Ion pairing would reduce the ionic strength to about 1.0 mol L^{-1}, with negligible effect on the activity coefficients of the reactants. As far as goodness of fit was concerned, the calculations of the kinetic parameters with allowance for ion pairing were generally poorer than those without. The effects of these somewhat arbitrary and computationally complex ion-pairing corrections are not large enough to warrant the choice of the adjusted results in preference to those derived directly from the stoichiometric cation concentrations; besides, any adjustment that results in an even more negative value for ΔV_0^* is suspect (see Discussion).

Discussion

The analysis of kinetic data, whether from NMR measurements or other techniques, for the manganate–permanganate OSET reaction is complicated by the difficulty of disentangling specific cation effects from Debye–Hückel and ion-association influences. In the present study, we have attempted to eliminate Debye–Hückel effects by maintaining constant ionic strength and have shown by calculation that ion pairing of the individual reactant ions with the counterions does not in itself complicate data analysis or vary greatly in importance from one alkali metal cation to another. What emerges is a linear dependence of k_{obsd} on [M$^+$] (eq 3); we follow precedent[11] in ascribing this to the existence of competing cation-dependent (k_M) and -independent (k_0) reaction pathways, but our finding that k_M is almost always dominant under practical experimental conditions, even for M = Li or Na, is a new result which has meant that the quantity of particular interest, k_0, is subject to large experimental uncertainties. Fortunately, k_0 becomes increasingly important as the pressure is raised, and satisfactory agreement between the variable-temperature and -pressure studies for various M$^+$'s confirms that the cation-independent pathway is properly characterized by the parameters $k_0 = 2.9 \times 10^3$ L mol^{-1} s^{-1}, $\Delta H_0^* = 46$ kJ mol^{-1}, $\Delta S^{0*} = -35$ J K^{-1} mol^{-1}, $\Delta V_0^{\circ *} = -23$ cm^3 mol^{-1}, and $\Delta\beta_0^* = -0.06$ cm^3 mol^{-1} MPa^{-1}, at 45 °C, 0.1 MPa, and ionic strength 1.1 mol L^{-1}. We attempt below to account for these values in terms of standard theories of OSET reaction rates, after consideration of the significance of the M$^+$ effect.

Catalysis by Alkali Metal Ions. Rosseinsky et al.[27] remind us that the observed effects of ionic strength on ΔS^* for cation–cation OSET reactions generally show trends opposite to those predicted from the usual applications of Debye–Hückel theory, but they

(24) Fuoss, R. M. *J. Am. Chem. Soc.* **1958**, *80*, 5059.
(25) Owen, B. B.; Miller, R. C.; Milner, C. E.; Cogan, H. L. *J. Phys. Chem.* **1961**, *65*, 2065.
(26) Sørensen, T. S.; Sloth, P.; Schrøder, M. *Acta Chem. Scand., Ser A* **1984**, *A38*, 735.
(27) Rosseinsky, D. R.; Stead, K.; Coston, T. P. J.; Glidle, L. *J. Chem. Soc., Chem. Commun.* **1986**, 70.

show that the theory can account for the trends in the activation parameters surprisingly well if the highly charged transition state, but *not* the separated reacting ions, is assumed to engage in Bjerrum-type association with the counterions. Thus, a term $K_{IP}I$ or, for the more general case where the ionic strength $I \neq [M^+]$, $K_{IP}[M^+]$ is added to the Brønsted–Bjerrum–Christiansen expression describing the dependence of ln k_{obsd} on I, and K_{IP} is specifically identified with the ion association constant for the transition state–counterion pair. For the present case, where I is constant but $[M^+]$ varies, the appropriate expression becomes

$$k_{obsd} = k_0 \exp(K_{IP}[M^+]) \quad (7)$$

On this view, the influence of cations on the manganate–permanganate OSET rate could be taken to reflect a simple electrolyte effect on k_0, rather than a distinct mechanistic pathway. The distinction is in a sense semantic, since both views reduce to acknowledgment of the presence of a counterion in some, but not all, transition-state assemblages. The kinetic effects predicted by the Rosseinsky model, however, are important only at much lower ionic strengths and apply to more highly charged reactants than were used in the present study.

Thus, although the Rosseinsky model seems to be appropriate to describe anion effects at relatively low and variable ionic strengths on many cation–cation OSET reactions, explanation of the generally much more prominent effects of cations on anion–anion OSET rates[17,18,28] requires some specific catalytic intervention by M^+, probably through a combination of reduction of anion–anion repulsions and facilitation of actual electron transfer through a superexchange type of process;[29] the system presumably represents a special case of the broader problem of electron transfer at a distance.[30,31] The order of catalytic efficacy Li < Na < K < Rb ≪ Cs correlates with the polarizabilities of M^+ (cf. Dennis et al.[28]) or, alternatively, inversely with the *hydrated* radii of $M^+(aq)$. For example, for the M–Cl "DHEV-II" interionic distances (in pm) of Sørensen et al.,[26] we find an empirical relationship

$$\ln k_M = 5.625 + 125/(r_{DHEV\text{-}II} - 257) \quad (8)$$

which has the form expected for a purely Coulombic effect of M^+ in entering between the reacting anions to facilitate their close approach but which would imply an unrealistically small Mn–M–Mn distance in the transition state. Simple calculations of the effect of M^+ on the Coulombic work ΔG_{COUL}^* of bringing the reactants together, with reasonable single-ion radii for manganate and permanganate (280 pm) and aqueous M^+[26] and with either a linear or a triangular arrangement of the three ions in close contact, predict a range in k_M less than one-sixth of that found experimentally, Li through Cs.

A complete treatment of the M^+ catalysis problem would presumably include both Coulombic and superexchange-type calculations in addition to the usual OSET considerations. It should explain why ΔH_M^* is 13 kJ mol^{-1} less than ΔH_0^*, whence the gross catalytic effect, but is essentially the same for Li, Na, K, and Rb (solubility limitations precluded extension of our measurements to M = Cs), so that the trend in catalytic activity is largely entropic in origin. It should also explain why ΔV_{Na}^* and ΔV_K^* are respectively about 23 and 19 cm^3 mol^{-1} more positive than ΔV_0^*. It might be thought that these differences represent simply the volume ΔV_{desolv} gained when Na^+ and K^+ are desolvated to give the shortest possible Mn–Mn distance in a transition state of the form $MnO_4^-\cdots M^+\cdots MnO_4^{2-}$. For total desolvation of aqueous M^+, a lower limit for ΔV_{desolv} can be established from the volume V_{core} of a mole of closest packed M^+ of ionic radius appropriate to the coordination number in solution[32,33] and the "absolute" molar volume of $M^+(aq)$ (=its conventional molar volume V_M° plus V_H° for $H^+(aq)$, here taken as −5.4 cm^3 mol^{-1} [34]):

$$\Delta V_{desolv} = V_{core} - (V_M^\circ + V_H^\circ) \quad (9)$$

For Na^+ and K^+, the calculated ΔV_{desolv} values are +10.3 and +8.1 cm^3 mol^{-1}, respectively—less than half the experimental ($\Delta V_M^* - \Delta V_0^*$). This may mean that the use of a closest packed volume for V_{core} is inappropriate but, more likely, desolvation of M^+ is not the only component of the measured ($\Delta V_M^* - \Delta V_0^*$). We shall see (below) that it seems necessary to modify the usual "two-sphere" model of OSET[2-6] by inclusion of ellipsoidal-cavity and/or nonadiabatic effects, in order to rationalize the strongly negative experimental value of $\Delta V_0^{\circ *}$. If, however, the role of M^+ is to make electron transfer between MnO_4^- and MnO_4^{2-} efficient over relatively wide Mn–Mn separations, neither the ellipsoidal-cavity model nor nonadiabaticity is likely to be relevant to the M^+-catalyzed path. Desolvation of M^+ would then account adequately for ΔV_M^* relative to a calculated "two-sphere" value for ΔV_0^* (i.e., +3 and −1 as against about −10 cm^3 mol^{-1}).

Cation-Independent Pathway: Rationalization of Activation Parameters. The classical, two-sphere Marcus–Hush theories of OSET reaction rates,[3-6,35,36] in simple terms, give the free energy of activation of ΔG^*

$$k_0 = (\varkappa k_B T/h) \exp(-\Delta G^*/RT) \quad (10)$$

as the sum of calculable contributions from the internal rearrangement of the two reacting molecules (ΔG_{IR}^*; Sham and Brunschwig's value[15] of 6.7 kJ mol^{-1} is used in the following calculations), the rearrangement of the surrounding solvent (ΔG_{SR}^*), the Coulombic work required to bring the reactants together (ΔG_{COUL}^*), and Debye–Hückel or other thermodynamic electrolyte effects (ΔG_{DH}^*); in the absence of electronic effects (i.e., if electron transfer is adiabatic[35,36]), the transmission coefficient $\varkappa$ is taken as unity.

$$\Delta G^* = \Delta G_{IR}^* + \Delta G_{SR}^* + \Delta G_{COUL}^* + \Delta G_{DH}^* \quad (11)$$

Stranks[2] differentiated the components of eq 11 with respect to pressure to obtain an analogous expression for the volume of activation:

$$\Delta V^* = \Delta V_{IR} + \Delta V_{SR}^* + \Delta V_{COUL}^* + \Delta V_{DH}^* \quad (12)$$

Similarly, differentiation of the negative of the terms in eq 11 with respect to temperature gives the corresponding entropies of activation:

$$\Delta S^* = \Delta S_{IR}^* + \Delta S_{SR}^* + \Delta S_{COUL}^* + \Delta S_{DH}^* \quad (13)$$

For the cation-independent manganate–permanganate OSET reaction, however, the simple classical two-sphere approach gives adiabatic reaction rates that are some 1000-fold too large[4] and a ΔV_0^* about 15 cm^3 mol^{-1} too positive.[9] We have shown elsewhere[7,8] how Stranks' equations for the components of eq 12 may be modified to generate ΔV_0^* values in better accord with experiment. We now report the results of an extensive reworking of those calculations with minor adjustments (e.g., P is set to 0.1 MPa throughout), investigation of the effects of varying parameters such as the ionic radii, and, most importantly, the constraint that an acceptable model must accommodate the experimental k_0, ΔS_0^*, and ΔH_0^* (=$\Delta G_0^* + T\Delta S_0^*$) as well as $\Delta V_0^{\circ *}$. The relevant expressions are given in the Appendix.

Adiabatic Two-Sphere Model: Variable Mn–Mn Separation. In most current models,[35,36] electron transfer is considered to occur over a *range* $\delta\sigma$ of Mn–Mn separations with maximum probability at a separation σ, rather than, as formerly supposed, at a fixed encounter distance (which was usually taken to be the sum (r_1

(28) Dennis, C. R.; Leipoldt, J. G.; Basson, S. S.; Van Wyk, A. J. *Inorg. Chem.* **1986**, *25*, 1268.
(29) McConnell, H. M. *J. Chem. Phys.* **1961**, *35*, 508.
(30) Guarr, T.; McLendon, G. *Coord. Chem. Rev.* **1985**, *68*, 1.
(31) Mayo, S. L.; Ellis, W. R., Jr.; Crutchley, R. J.; Gray, H. B. *Science (Washington, D.C.)* **1986**, *233*, 948.
(32) Swaddle, T. W.; Mak, M. K. S. *Can. J. Chem.* **1983**, *61*, 473.
(33) Shannon, R. D. *Acta Crystallogr., Sect. A: Cryst. Phys., Diffr., Theor. Gen. Crystallogr.* **1976**, *A32*, 751.
(34) Millero, F. J. In *Water and Aqueous Solutions*; Horne, R. A., Ed.; Wiley-Interscience: New York, 1972; Chapter 13.
(35) Sutin, N. *Prog. Inorg. Chem.* **1983**, *30*, 441.
(36) Newton, M. D.; Sutin, N. *Annu. Rev. Phys. Chem.* **1984**, *35*, 437.

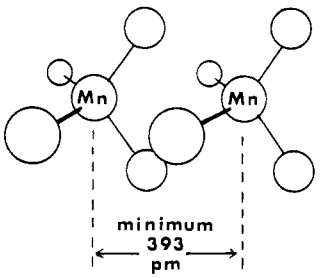

Figure 3. Mode of approach of manganate and permanganate ions to achieve minimal Mn–Mn separation.

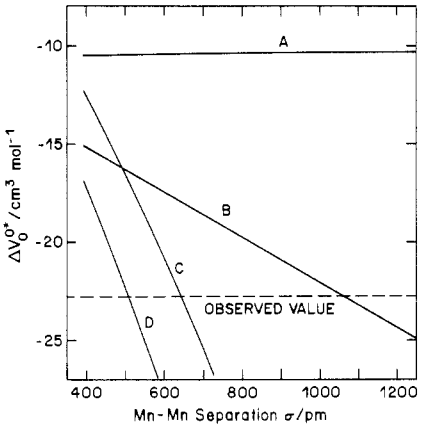

Figure 4. Calculated dependence of volume of activation for the cation-independent reaction pathway on the Mn–Mn distance σ (σ assumed to be pressure-dependent); at 45 °C, 0.1 MPa, ionic strength 1.1 mol L^{-1}, and $r_1 = r_2 = 280$ pm: (A) adiabatic two-sphere model; (B) nonadiabatic two-sphere model; (C) adiabatic ellipsoidal-cavity model; (D) nonadiabatic ellipsoidal-cavity model.

$+ r_2$) of the effective radii of the reactants). If so, then the effect of pressure on σ must be allowed for in evaluating eq 12 (eq 11 is not affected). We avoid the serious difficulties this entails by assuming that the assemblage of reactants compresses as does the surrounding medium, so that $-\sigma^{-1}(\partial\sigma/\partial P)_T = \beta/3$, where β is the isothermal compressibility of the solvent.[7,8] The assumption that σ is pressure-dependent is incorporated in all the models considered in this paper.

A secondary consequence of this assumption, omitted from our previous calculations,[7-9] is the effect of pressure on the factor $4000\pi N\sigma^3/3$ (where $\sigma \simeq r_1 + r_2$, in meters) in the precursor formation constant expression;[35,36] this makes $\Delta V_0{}^{o*}$ more *positive* by an amount $RT\beta$ or 1.1 cm^3 mol^{-1}. Furthermore, interpenetration of the oxo ligands[37] (Figure 3) could permit electron transfer at Mn–Mn separations down to 393 pm; thus, σ is subject to compression even when the reactants, approximated to spheres in the customary way, are "in contact" (in this case, at $\sigma = r_1 + r_2 = 560$ pm[8]). The net effect of allowing σ to vary with pressure is to make $\Delta V_0{}^*$ for the two-sphere model about 4 cm^3 mol^{-1} more negative (though almost independent of pressure in itself), but still about 12 cm^3 mol^{-1} more positive than the experimental value (Figure 4). Adoption of Kharkats' modification of the two-sphere model,[38] which allows (inter alia) for the solvent "cut out" by the other ion in an encounter, led only to a negligibly small (+0.7 cm^3 mol^{-1}) effect on $\Delta V_0{}^*$.

If both σ and r ($=r_1 = r_2$) are allowed to vary simultaneously, k_0 (which is very sensitive to σ as well as r) and $\Delta V_0{}^*$ both equal the experimental values when $r = 142$ pm and $\sigma = 170$ pm, but these results can have no physical meaning. Thus, the adiabatic two-sphere model cannot accommodate the experimental data under any realistic conditions.

Nonadiabatic Two-Sphere Model. If the electron transfer is nonadiabatic, as German[16] has suggested, $\Delta V_0{}^{o*}$ calculated on the two-sphere model (with distance scaling parameter $\alpha = 1.5 \times 10^{10}$ m^{-1} [16,35]) becomes more negative as σ increases but reaches the experimental value of -23 cm^3 mol^{-1} only at very long range (σ = 1050–1100 pm). This corresponds to the time-averaged distance between the reactant anions at standard-state concentrations, implying that nonadiabatic OSET occurs continuously at long range without the need for close encounters. Electron transfer can, in some circumstances, be quite rapid at ranges even longer than this,[31] but this seems unlikely in the present case, especially since Rosseinsky[39] finds that Mn–Mn electron transfer at σ on the order of 500 pm in solid $K_3(MnO_4)_2$ occurs at rates similar to those found in solution. Furthermore, although the simple Marcus–Hush model "correctly" predicts $k_0 = 2800$ L mol^{-1} s^{-1} at 45 °C for $\sigma = 1080$ pm, this requires *fully adiabatic* OSET, so the two-sphere, long-range, nonadiabatic model must be rejected. More sophisticated calculations by German,[16] using the theory of nonadiabatic transitions, give k_0 values satisfactorily close to the experimental ones at 298 K with σ = 600–650 pm, but the predicted $\Delta H_0{}^*$ and $|\Delta V_0{}^{o*}|$ are too low.

The question of nonadiabaticity in redox reactions in general is currently unsettled;[40-42] for the manganate–permanganate OSET reaction, the Mn–O bond lengths[15] and the electronic structures of the reactants are so similar that significant departures from adiabaticity seem unlikely,[42] but our naive calculations using Slater 3d radial functions suggest that, if the hexaaquairon(II/III) OSET reaction is not fully adiabatic except at $\sigma < (r_1 + r_2)$,[36] the same may hold true for the manganate(VI/VII) case.

Ellipsoidal-Cavity Models. Adiabaticity apart, it is the solvent rearrangement term that dominates both $\Delta V_0{}^*$ and $\Delta G_0{}^*$. The manganate and permanganate ions are small relative to the reactants normally considered in OSET studies, and the shortcomings of the various two-sphere models may arise in this case because the solvent should not be treated as a continuous, structureless dielectric in a close manganate–permanganate encounter, although this seems to be an acceptable approximation for larger reactants[43] (and possibly also for the M^+-catalyzed case, as noted above). The problem lies, not with dielectric saturation near the ions (adaptation of Abe's[44] equation, which allows the dielectric constant to rise exponentially to the bulk solvent value D as the distance from the ion increases, gave unwieldy equations and generally more *positive* values of $\Delta V_0{}^*$ than with constant D), but rather with the expulsion of water molecules from the interionic region.

Cannon[45] has proposed a model (originally intended primarily to deal with intramolecular-electron-transfer rates) in which the reacting entities, in the transition state, are enclosed in an ellipsoidal cavity in the solvent. This model has some significant defects[46,47] but nevertheless provides a marked improvement over the two-sphere alternatives in the calculation of realistic solvent reorganization contributions to eq 11 and 12, and we will continue to use our adaptations[7,8] of the Cannon equation[45] until the recently announced[47] more tractable version of the Brunschwig–Ehrenson–Sutin treatment is published.

The major and minor semiaxes of the ellipsoidal cavity may be taken to be $(r + \sigma/2)$ and r, respectively ($r = r_1 = r_2 = 280$ pm); this amounts to assuming that the volume of the ellipsoid is the sum of the effective spherical volumes of the MnO_4 units when $\sigma = 2r$. The impact of the ellipsoidal-cavity assumption on the work terms has been ignored, as it takes effect only at very short range, and besides the work terms are not major contributors

(37) Logan, J.; Newton, M. D. *J. Chem. Phys.* **1983**, *78*, 4086.
(38) Kharkats, Yu, I. *Sov. Electrochem. (Engl. Transl.)* **1976**, *12*, 566.
(39) Rosseinsky, D. R.; Stephan, J. A.; Tonge, J. S. *J. Chem. Soc., Faraday Trans. 1* **1981**, *77*, 1719. Rosseinsky, D. R.; Tonge, J. S. *Ibid.* **1982**, *78*, 3595. The Mn–Mn distance cited in these papers is incorrect (personal communication from D. R. Rosseinsky).
(40) Balzani, V.; Scandola, F. *Inorg. Chem.* **1986**, *25*, 4457.
(41) Furholz, U.; Haim, A. *Inorg. Chem.* **1985**, *24*, 3091.
(42) Ramasami, T.; Endicott, J. F. *Inorg. Chem.* **1984**, *23*, 3324; *J. Am. Chem. Soc.* **1985**, *107*, 389.
(43) Hupp, J. T.; Weaver, M. J. *J. Phys. Chem.* **1985**, *89*, 1601.
(44) Abe, T. *J. Phys. Chem.* **1986**, *90*, 713.
(45) Cannon, R. D. *Chem. Phys. Lett.* **1977**, *49*, 299.
(46) German, E. D.; Kuznetsov, A. M. *Electrochim. Acta* **1981**, *26*, 1595.
(47) Brunschwig, B.; Ehrenson, S.; Sutin, N. *J. Phys. Chem.* **1986**, *90*, 3657.

to ΔV_0^*. For adiabatic OSET on the adapted Cannon model, $\Delta V_0^{\circ *}$ would reach the experimental value at σ = 640 pm, but the calculated k_0 is then 30-fold too small, and besides this is not a sufficiently close approach to justify resort to the ellipsoidal-cavity model. The experimental value of k_0 corresponds to a very reasonable σ = 550 pm, for which $\Delta V_0^{\circ *}$ is predicted to be −19 $cm^3\ mol^{-1}$ (Figure 4)—slightly less than the "best" experimental value but certainly acceptable in view of the problems in measuring the cation-independent OSET rates. Most encouragingly, the adiabatic ellipsoidal-cavity model predicts $\Delta S_0^* = -37.3$ J K^{-1} mol^{-1} and $\Delta H_0^* = 45.2$ kJ mol^{-1}, which match the observed values to well within experimental uncertainty. For the adiabatic two-sphere model with the same σ and r, the corresponding predictions are −30.5 J K^{-1} mol^{-1} and 34.2 kJ mol^{-1}, with $k_0 \simeq 4.1 \times 10^5$ L mol^{-1} s^{-1}; thus, the chief effect of introducing the solvent-cavity assumption is to slow OSET down by at least 2 orders of magnitude, largely through increasing ΔH_0^*, and to make ΔV_0^* sharply dependent upon σ (Figure 4).

If OSET is *non*adiabatic, the ellipsoidal-cavity model generates the experimental value of $\Delta V_0^{\circ *}$ exactly when σ = 510 pm, which corresponds to a modest degree of interpenetration of the oxo ligands as in Figure 3. For this configuration, we calculate $k_0 \simeq 1.1 \times 10^4$ L mol^{-1} s^{-1} (corresponding to $\varkappa \simeq 0.26$), $\Delta S_0^* = -39$ J K^{-1} mol^{-1}, and $\Delta H_0^* = 41$ kJ mol^{-1}. Thus, an adiabatic or slightly nonadiabatic ellipsoidal-cavity model explains the experimental data very well.

Pressure Dependence of the Volume of Activation. All of the above models predict that ΔV_0^* will become less negative as the pressure increases, because parameters such as β and the pressure derivatives of the refractive index and the dielectric constant themselves become numerically smaller. In general, ΔV_0^* is predicted to be roughly 4 $cm^3\ mol^{-1}$ more positive at 100 MPa than at 0.1 MPa ($\Delta\beta_0^* \simeq -0.06$ to -0.10 $cm^3\ mol^{-1}\ MPa^{-1}$ but not necessarily constant), which is in accordance with the results of analysis of the experimental data according to eq 6. Conversely, the need to allow for some pressure dependence of ΔV_0^* during statistical analysis is made clear.

Conclusion. The activation parameters for the cation-independent path for OSET between manganate and permanganate ions in aqueous alkali are well represented by a modified Marcus–Hush type model in which the pressure (and temperature) dependence of the most favorable Mn–Mn separation is acknowledged and the reactants are considered to be enclosed in a common cavity (expediently taken to be ellipsoidal) in the solvent. The smallness of the reactant ions may account for the need to invoke the solvent-cavity model; this may be unnecessary for OSET reactions of larger ions. The effect of this solvational arrangement is to make OSET slower, ΔH_0^* larger, and the entropy and volume of activation more negative, relative to the predictions of conventional "two-sphere" (continuous dielectric) models. Improvements[46,47] to the Cannon ellipsoidal-cavity model[45] are unlikely to change these general conclusions significantly. The efficacy of M^+ (M = Li < Na < K < Rb < Cs) in catalyzing the reaction through reducing ΔH_M^*, and in making ΔV_M^* much more positive than ΔV_0^*, may originate at least partially in a relaxation of these solvational constraints.

Acknowledgment. We thank Drs. E. D. German, M. D. Newton, and D. R. Rosseinsky for correspondence and the Natural Sciences and Engineering Research Council of Canada for financial assistance.

Appendix: Components of Eq 11, 12, and 13

In the following equations, D is the relative permittivity (dielectric constant), n the refractive index, β the isothermal compressibility, γ the thermal expansivity ($V^{-1}(\partial V/\partial T)_P$), and ρ the density of the solvent; a, B, and C are the Debye–Hückel parameters; $S(\lambda_0)$ is the shape factor defined by Cannon;[45] α is the nonadiabatic distance scaling parameter, taken to be 15 nm^{-1};[16,35] and the remaining symbols have their usual SI meaning or are defined above. The Mn–Mn separation σ is assumed to compress as does the solvent (in one dimension), and the effective radii[8,32] r_1 and r_2 of the reactant anions are taken to be equal (r). The charges on the reactants are Z_1 and Z_2.

(A) Adiabatic Two-Sphere Model. $\Delta G_{IR}^* = 6.7$ kJ mol^{-1};[15] $\Delta V_{IR}^* \sim 0$;[2,7-9] $\Delta S_{IR}^* \sim 0$.

$$\Delta G_{SR}^* = (Ne^2/16\pi\epsilon_0)(n^{-2} - D^{-1})(r^{-1} - \sigma^{-1}) \quad (14)$$

$$\Delta V_{SR}^* = (Ne^2/16\pi\epsilon_0)[(r^{-1} - \sigma^{-1}) \times (\partial(n^{-2} - D^{-1})/\partial P)_T - (n^{-2} - D^{-1})\beta/3\sigma] \quad (15)$$

$$\Delta S_{SR}^* = -(Ne^2/16\pi\epsilon_0)[(r^{-1} - \sigma^{-1}) \times (\partial(n^{-2} - D^{-1})/\partial T)_P + (n^{-2} - D^{-1})\gamma/3\sigma] \quad (16)$$

$$\Delta G_{COUL}^* = NZ_1Z_2e^2/4\pi\epsilon_0 D\sigma \quad (17)$$

$$\Delta V_{COUL}^* = (NZ_1Z_2e^2/4\pi\epsilon_0\sigma)[(\partial D^{-1}/\partial P)_T + \beta/3D] \quad (18)$$

$$\Delta S_{COUL}^* = -(NZ_1Z_2e^2/4\pi\epsilon_0\sigma D)[(\gamma/3) - (\partial \ln D/\partial T)_P] \quad (19)$$

$$\Delta G_{DH}^* = 2RTZ_1Z_2CI^{1/2}/(1 + BaI^{1/2}) \quad (20)$$

$$\Delta V_{DH}^* = \frac{RTZ_1Z_2CI_{1/2}}{(1 + BaI^{1/2})^2}\left[\left(\frac{\partial \ln D}{\partial P}\right)_T(3 + 2BaI^{1/2}) - \beta\right] \quad (21)$$

$$\Delta S_{DH}^* = \frac{2Z_1Z_2RTI^{1/2}}{(1 + BaI^{1/2})^2}\left[(1 + BaI^{1/2})\left(\frac{\partial C}{\partial T}\right)_P - aCI^{1/2}\left(\frac{\partial B}{\partial T}\right)_P\right] \quad (22)$$

where

$$(\partial C/\partial T)_P = -(C/2)[\gamma + 3(T^{-1} + (\partial \ln D/\partial T)_P)] \quad (23)$$

and

$$(\partial B/\partial T)_P = -\frac{e}{2}\left(\frac{2N\rho}{\epsilon_0 k_B DT}\right)^{1/2}[\gamma + T^{-1} + (\partial \ln D/\partial T)_P] \quad (24)$$

The cation–anion closest approach distance a is taken to be 350 pm, by analogy with $MClO_4$.[26] The pressure and temperature dependences of the preexponential factor $4000\pi N\sigma^3/3$ in the work terms contribute $+RT\beta$ and $-RT\gamma$ to the values of ΔV_0^* and ΔS_0^*, respectively.

(B) Nonadiabatic Two-Sphere Model. As for (A), but transmission coefficient $\varkappa < 1.0$, and the following term is added on the right of eq 12. The effect of thermal expansion of σ on $\varkappa$ is neglected.

$$\Delta V_{NA}^* = -2RT\alpha\beta\sigma/3 \quad (25)$$

(C) Adiabatic Ellipsoidal-Cavity Model. As for (A), but eq 14–16 are replaced by eq 26–28, respectively. The pressure and temperature dependences of $S(\lambda_0)$ are negligible.

$$\Delta G_{SR(ELL)}^* = Ne^2\sigma^2S(\lambda_0)(n^{-2} - D^{-1})/32\pi\epsilon_0 r^2(r + \sigma/2) \quad (26)$$

$$\Delta V_{SR(ELL)}^* = [Ne^2\sigma^2S(\lambda_0)/16\pi\epsilon_0 r^2(2r + \sigma)] \times [(\partial(n^{-2} - D^{-1})/\partial P)_T - (\sigma + 4r)(n^{-2} - D^{-1})\beta/3(2r + \sigma)] \quad (27)$$

$$\Delta S_{SR(ELL)}^* = -\frac{Ne^2\sigma^2S(\lambda_0)}{16\pi\epsilon_0 r^2(2r + \sigma)}[(\partial(n^{-2} - D^{-1})/\partial T)_P + \gamma(4r + \sigma)(n^{-2} - D^{-1})/3(2r + \sigma)] \quad (28)$$

(D) Nonadiabatic Ellipsoidal-Cavity Model. As for (C), but with the addition of eq 25; $\varkappa < 1$.

Registry No. MnO_4^-, 14333-13-2; MnO_4^{2-}, 14333-14-3; Li, 7439-93-2; Na, 7440-23-5; K, 7440-09-7; Rb, 7440-17-7.

Supplementary Material Available: Tables showing the temperature dependence of rate constants k_{obsd}, k_0, and k_M (M = Li, Na, K, Rb) and pressure dependence of k_{obsd} (M = Na, K) (7 pages). Ordering information is given on any current masthead page.